Langmuir

Article

pubs.acs.org/Langmuir

Preparation and Characterization of Alkylphosphonic Acid Self-Assembled Monolayers on Titanium Alloy by Chemisorption and Electrochemical Deposition

Noah Metoki,[†] Liang Liu,[§] Edith Beilis,[∥] Noam Eliaz,[†] and Daniel Mandler*[,§]

[†]Biomaterials and Corrosion Lab, Department of Materials Science and Engineering, Tel-Aviv University, Ramat Aviv 6997801, Israel

[§]Institute of Chemistry, The Hebrew University of Jerusalem, Jerusalem 91904, Israel

[∥]Center for Nanoscience and Nanotechnology, Tel-Aviv University, Ramat Aviv 6997801, Israel

Supporting Information

ABSTRACT: Ti-6Al-4V alloy is the most commonly used alloy for dental and orthopedic implants. In order to improve osseointegration, different surface modification methods are usually employed, including self-assembled monolayers (SAMs). This study presents an investigation of both active (electro-assisted) and passive (adsorption) approaches for the modification of Ti-6Al-4V using alkylphosphonic acid. The monolayers were characterized by cyclic voltammetry, double-layer capacitance, contact angle measurements, X-ray photoelectron spectroscopy, polarization modulation infrared reflection adsorption spectroscopy, electrochemical impedance spectroscopy, and corrosion potentiodynamic polarization measurements. It is shown that the electrochemically assisted monolayers, which are assembled faster, exhibit better control over surface properties, a superior degree of order, and a somewhat higher packing density. The electrosorbed SAMs also exhibit better blockage of electron transfer across the interface and thus have better corrosion resistance.

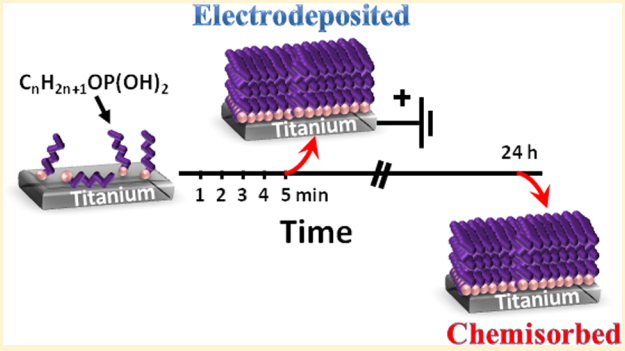

INTRODUCTION

Titanium and its alloys (mostly Ti-6Al-4V and Ti-6Al-4Nb) have been widely used in orthopedic and dental surgery for decades due to their superior properties.[1,2] Specific advantages include low density (ρ = 4.51 g/cm^3), biological and chemical inertness, low electrical and thermal conductivity ($\sigma = 2.3 \times 10^4$ 1/(Ω·cm) at 22 °C, κ = 22 W/(m·K) at 27 °C, respectively), a relatively low modulus of elasticity (110 GPa) that reduces the risk of stress shielding, and good fatigue strength (300 MPa at 10^7 cycles).[3] The oxide layer on commercially pure titanium and on Ti-6Al-4V is very similar, varying only by the small concentration of the α-phase stabilized by aluminum.[4] Titanium and its alloys generally exhibit good biocompatibility and osseointegration properties. However, the osseointegration of a titanium implant depends on several factors, including biorecognition, bone growth and adhesion of the newly forming bone at the implant surface.[5,6] Consequently, improvement in the biological, chemical, and mechanical properties is often accomplished by surface modification using different approaches. The latter can be divided into surface treatment and coating, whereby inorganic and organic matrices including polymers are utilized.[7]

An attractive approach to modifying the interfacial properties of Ti and its alloys is by self-assembled monolayers (SAMs). These are easy to manipulate and allow one to control the surface composition and thus the implant bioactivity and biocompatibility at relatively low cost. Accordingly, the interest and effort in SAMs related to titanium have constantly increased and have resulted in numerous reports.[8−26] The most commonly studied SAMs on titanium surfaces have been alkoxy- and chlorosilanes and carboxylic, phosphonic, and phosphoric-terminated acids which bond to the oxide surface using OH groups.[9−17,27] Hähner et al.[18] studied alkanephosphates on metal oxides including titanium oxide and found that these produce oriented, well-ordered films that show no dependence on the preparation conditions as long as the surface roughness is low. It was concluded to have coverage comparable to that of long-chain thiols on gold. More recently, HailuTaffa et al.[19] showed that the interfacial properties of the surface, such as wettability and ion exchange, could be tuned by modifying the headgroups of alkylphosphonic acids. It was discovered that the layers reach a stable surface coverage within days. Balahur et al.[20] demonstrated that the wettability of a TiO_2 surface coated with silane SAM could be well controlled by UV irradiation. Evidently, the formation of these SAMs on Ti involves a strong interaction between a functional group and

Received: December 17, 2013
Revised: May 3, 2014

   dx.doi.org/10.1021/la404829b | Langmuir XXXX, XXX, XXX−XXX

the oxide surface that allows hydrolysis. Yet, there is much difference between them; Adolphi et al.[27] found that phosphonic acids bind more strongly to the metal oxides than do carboxylic acids. Silverman et al.[28] showed the superiority of the phosphonate interface with titanium at physiological pH in comparison to silane functional groups. These SAMs are often designed with a functional end-group, which can be linked to proteins and cells or even induce the growth of coatings such as calcium phosphate.[21,22]

A literature survey reveals that typically the assembly method comprises a passive adsorption mechanism by which the substrate is either immersed in the surfactant solution or exposed to its vapors during a predefined, relatively long period of time (typically 24 h).[9,23−25] In this study, a much faster active approach based on the application of an electrochemical potential for a short time is studied and compared with the conventional approach. This electrochemical method induces organization and allows us to control the molecular assembly at the interface.

Electroassisted adsorption of thiols on Au, Ag, and Hg from alkaline aqueous solutions has been reported.[29−32] Related studies carried out on gold surfaces have highlighted the major improvement in the structure, organization, and protection of mostly alkanethiol monolayers assembled under electrochemical potential. High-quality SAMs have been generated with a significant savings of time with regard to the passive approach.[29,33,34] Recently, few studies have been devoted to the electroassisted assembly of organothiols and other ω-functionalized alkanes on oxidizable metals and alloys, such as nickel,[35] carbon steel,[36−38] and copper.[39,40] To the best of our knowledge, the only study that deals with the electroassisted formation of SAM on titanium was reported by Oya et al.,[41] who claimed to electrochemically immobilize Arg-Gly-Asp (RGD) molecules on a titanium surface by applying a potential. However, no additional details were provided.

This study presents an investigation of both active (electroassisted) and passive (adsorption) approaches for the modification of titanium alloy (Ti-6Al-4V) using alkylphosphonic acid. The formation of highly reproducible, stable, well-ordered, and closely packed monolayers is shown.

EXPERIMENTAL SECTION

Chemicals. Hexylphosphonic acid (95%), decylphosphonic acid (97%), tetradecylphosphonic acid (97%), hexadecylphosphonic acid (97%), hexaammineruthenium(III) trichloride (98%), potassium nitrate (99%), and phosphate-buffered saline (PBS) were purchased from Sigma-Aldrich. Ti-6Al-4V ELI grade (ASTM F136-02a) rods, 0.5 in. long and 0.2 in. in diameter, were produced by Dynamet Inc. (Washington, PA) and supplied by Barmil (Petach-Tikva, Israel). The 0.2-inch rods were embedded in a Teflon sheath, exposing only the a disk that served as the electrode surface. Deionized (DI) water (>18 MΩ·cm^{-1}) was used for all experiments.

Instruments. Electrochemical measurements were conducted with a PAR-263A potentiostat/galvanostat operating in potentiostatic mode, using a three-electrode cell with a saturated Ag/AgCl reference electrode (RE) and a platinum counter electrode (1 cm^2 in area). Electrochemical deposition and electrochemical impedance spectroscopy (EIS) were carried out with a potentiostat (CHI-750B, CH Instruments Inc., TX, USA) using a single-compartment three-electrode glass cell. The same RE was used for these experiments; therefore, all potentials are quoted hereafter vs this RE. For these experiments, a 5-mm-diameter graphite rod was used as a counter electrode.

Contact angle measurements were conducted using Ramé-Hart model 100 contact angle goniometer. Advancing and receding contact angles were determined by adding and withdrawing a fixed amount of DI water to and from the drop, respectively. The values reported here are the averages of three measurements performed on each sample.

Polarization modulation infrared reflection absorption spectroscopy (PM-IRRAS) spectra were recorded using Bruker optics PMA50 external module in conjunction with a Vertex 70 Fourier transform infrared (FTIR) spectrometer. A liquid-nitrogen-cooled MCT detector was used in all experiments. Samples of evaporated titanium on glass covered with SAMs were mounted in the PMA50 sample holder. The incident beam angle used in all experiments was 85°. The wavelength setting on a Hinds PEM90 was fixed at 2600 cm^{-1} with a half-wave retardation of 0.5. Lock-in amplifier (LIA) SR830 settings were used according to the PMA50 manual, except for the sensitivity which was set to 50 mV. The samples were scanned for 25 min with 4 cm^{-1} resolution and an aperture of 1.5 mm depending on the PM-IRRAS signal. The resulting absorption spectra were recorded between 800 and 4000 cm^{-1}. Conversion of the resulting interferograms to raw PM-IRRAS spectra was performed using the VisualBasic script included in Bruker OPUS spectroscopy V.5.5 software. The analysis of the raw PM-IRRAS spectra, including the removal of the background, y-scale normalization, and removal of the LIA gain factor, was based on section V.4.E of the PMA50 manual.

X-ray photoelectron spectroscopy (XPS, AXIS ULTRA, Kratos Analytical Ltd., Manchester, U.K.) measurements were acquired with monochromated Al Kα (1486.7 eV), and high-resolution scans were collected for Au 4f peaks with a 20 eV pass energy.

Procedures. For the chemisorption of SAMs, the titanium alloy rods were machined into 1- and 2.5-cm-long samples. These electrodes were cleaned in acetone and ground on silicon carbide papers (P600, P1000), followed by fine polishing with alumina paste (down to 0.05 μm) on a microcloth polishing pad and washed with DI water and acetone alternately. Chemical etching was followed by dipping the sample in an HF (40%)/HNO_3 (65%) solution (2 and 20 vol %, respectively) for 2 min and then dipping three times in DI water at ambient temperature. The samples were then immediately immersed in a 1 mM solution of the alkylphosphonic acid in DI water for 24 h (hexadecylphosphonic acid solution was added to NaOH (2 mM) in order to dissolve the powder better). This was followed by dipping the samples three times in DI water at ambient temperature, gently washing in running DI water, and drying in argon.

For the electrodeposition of SAMs, the 0.2-in.-diameter rods were embedded in Teflon and cleaned and polished in the same manner. After 24 h of exposure to air at room temperature, the samples were immersed in a 1 mM solution of the alkylphosphonic acid and 0.01 M KNO_3 in DI water under a potential of +1.2 V vs Ag/AgCl for 250 s. Afterward, the samples were rinsed gently with DI water and dried in argon.

Cyclic voltammetry (CV) was performed in 1 mM $Ru(NH_3)_6^{3+}$ and 0.1 M KNO_3 between 0.4 and −0.4 V at a scan rate of 20 mV/s. The double-layer capacitance, C_{dl}, was determined from the CV by cycling the electrodes in the non-Faradaic region at different scan rates in a solution of 0.1 M KNO_3. EIS was conducted in a solution containing equal concentrations of $Fe(CN)_6^{3-}$/$Fe(CN)_6^{4-}$ (1 mM each) using a three-electrode cell, as described earlier for the chemisorbed and electrochemically prepared electrodes. The impedance data were analyzed with Zview impedance analysis software (Scribner Associates, Inc., Southern Pines, NC). All measurements were performed at room temperature (21 ± 2 °C).

Corrosion tests were performed using 0.5-in.-diameter rods cleaned and polished in the same manner. The samples were immersed in a three-electrode cell containing PBS with a saturated calomel reference electrode (SCE) connected by a salt bridge. The bath was maintained at 37 ± 1 °C by means of a Lauda E-220T Ecoline thermostatic bath. The polarization experiments were conducted starting from a value −100 mV more cathodic than the open-circuit potential (that was measured for 1 h) and sweeping the potential in the anodic direction and back at 0.167 mV/s. The solution was dearated with nitrogen 1 h before the experiment and through the duration of the experiment.

dx.doi.org/10.1021/la404829b | Langmuir XXXX, XXX, XXX−XXX

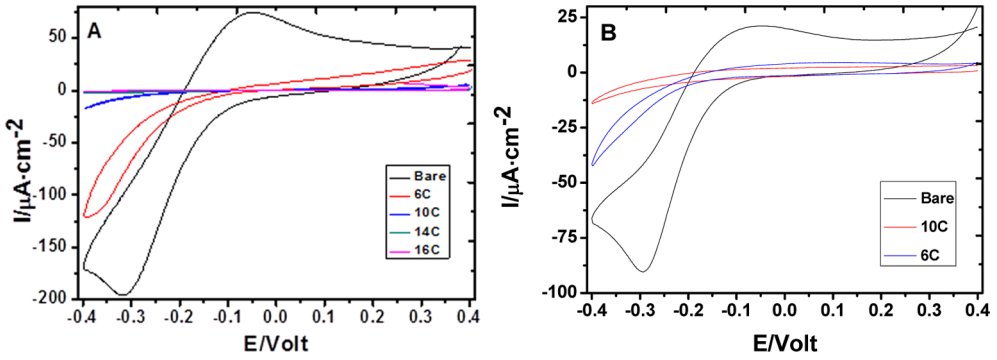

Figure 1. Cyclic voltammetry of Ti-6Al-4V electrode recorded in a 1 mM $Ru(NH_3)_6^{3+}$ solution consisting of 0.1 M KCl (20 mV/s) (A) chemisorbed and (B) electrochemically formed. 6C, 10C, 14C, and 16C stand for hexylphosphonic acid, decylphosphonic acid, tetradecylphosphonic acid, and hexadecylphosphonic acid, respectively.

RESULTS AND DISCUSSION

Electroassisted adsorption of SAMs is a relatively new concept unexplored for reactive metals, such as titanium. This process, which involves applying positive potentials, is complex since it needs to take into account the interaction between the amphiphiles and the potential-dependent oxide layer. Previous studies have shown that electroassisted SAMs were formed much faster and exhibited superior organization.[33,42] Hence, our principal motivation to form SAMs electrochemically on titanium has been driven by superior control over surface coverage and time savings. Below we describe and compare the formation of well-ordered SAMs of homologous alkylphosphonic acids on titanium alloy by chemisorption and a step potential.

Figure 1 shows the CV of Ti-6Al-4V coated with 1 mM $Ru(NH_3)_6^{3+}$ and 0.1 M KNO_3 with alkylphosphonic acids having different chain lengths. The SAMs were formed either by chemisorption (24 h) or electrochemically (1.2 V, 250 s). The figure shows only the first scan, as there is no significant change in the subsequent potential scans. The CV of a "bare" titanium electrode shows a quasi-reversible wave with ca. ΔE_{pk} = 0.24 V and a ratio of ca. 2.63 between the cathodic and anodic peak currents. The latter indicates that the reduction and oxidation of hexaammineruthenium(III) is not completely chemically reversible. Current densities in Figure 1A are higher than those in Figure 1B since an O-ring setup was used previously. In this type of setup, the working electrode is pressed against a doughnut-shaped ring to seal specific sections of the electrode and create a defined surface area for the experiment. Yet, this setup does not define the surface area well; therefore, a deviation in the current density can be observed. It is worth mentioning that under these conditions a native oxide layer covers the electrode surface. Previous reports suggested that the TiO_2 electrode behaves as an insulator rather than a metal under these conditions.[43,44] HailuTaffa et al. stated that the fact that the current density varied inversely with pH, yet was generally in the range expected for a flat gold electrode, suggests that $Ru(NH_3)_6^{3+}$ diffused through pores and charge transfer occurred at defects on TiO_2 exhibiting unexpected metallic behavior.[19]

The CV of the Ti alloy coated with an alkylphosphonic acid SAM clearly shows blocking behavior, which increased upon increasing the chain length of the monolayer. Blocking was estimated by the decrease in the peak current (measured at the peak potential) in comparison with that of a bare electrode. We found that blocking occurred to the same extent in both the chemisorbed and the electrochemically formed SAMs.

The electroassisted formation of hexylphosphonic acid and decylphosphonic acid on Ti-6Al-4V was thoroughly studied and optimized. Longer chain lengths were not investigated because of micelle formation in the aqueous solution, which made it difficult to assemble on the surface over a short period of time. The effects of solvent, electrolyte, time, potential, and concentration of the two alkylphosphonic acids were investigated. Figure 1S shows, for example, the effect of the applied potential (t = 250 s) on the electron-transfer blocking properties of the SAMs.

Table 1 lists the double-layer capacitance of the samples, both chemisorbed and electrochemically attached. The capacitance was derived from the CV, where a linear dependence between the non-Faradaic current and the scan rate was obtained. There is a significant difference between the control (bare) and the surfaces coated with the alkylphosphonic acids. The double layer can be described to a first approximation by the Helmholtz model (eq 1)

Table 1. Double-Layer Capacitance of Bare, Chemisorbed and Electrochemically Prepared Alkylphosphonic Acid SAMs on Titanium Surfaces[a]

	chemisorbed	electrochemically prepared
sample	capacitance [μF/cm^2]	capacitance [μF/cm^2]
control	39.25 ± 8.14	39.89 ± 1.06
6C	4.66 ± 1.60	5.42 ± 1.35
10C	2.98 ± 0.81	2.70 ± 0.27
14C	1.41 ± 0.22	
16C	1.05 ± 0.09	

[a]Values are presented as the mean ± standard deviation.

$$C_{dl} = \frac{\varepsilon \varepsilon_0 A}{d} \quad (1)$$

where ε is the dielectric constant, ε_0 is the permittivity of free space, A is the area of the working electrode, and d is the distance between the plates of the capacitor. Therefore, it is expected that the capacitance of the interface covered with a monolayer will decrease inversely with its thickness. Indeed, plotting the results of the chemisorbed samples shown in Table 1 as a function of the number of carbons in the alkylphosphonic chain (n, Figure 2) gives a straight line, where the dielectric constant can be determined from the slope. The calculated ε is

dx.doi.org/10.1021/la404829b | Langmuir XXXX, XXX, XXX−XXX

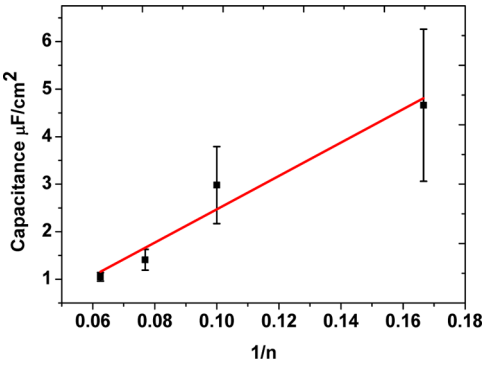

Figure 2. Double layer capacitance as a function of the inverse number of carbons in the alkylphosphonic chain.

ca. 7.9 ± 3.8, which is somewhat higher than the typical dielectric constant for pure alkylphosphonic acids (4.3−6.3[45]). This can be explained by recalling that our interface is a series of two capacitors representing the oxide layer and the organic film. Clearly, the Helmholtz model cannot account for these interfaces and a more elaborate approach must be applied using EIS vide infra. However, the clear resemblance that can be observed between the chemisorbed and the electrochemically prepared samples suggests that the electrochemically prepared samples also form a SAM, similar to that of the chemisorbed sample.

Further insight into the interface can be achieved by measuring the advancing and receding contact angles of a sessile water drop. Table 2 summarizes the average of three measurements performed on evaporated titanium surfaces. The latter were used to avoid the contribution of surface roughness.

Evidently, the contact angles of chemisorbed and electrochemically prepared Ti surfaces are significantly higher than that of the bare surface. The advancing contact angles vary between 86 and 108°, indicating the hydrophobic nature of the coated surfaces. Furthermore, a clear trend in increasing the advancing contact angles with the length of the alkylphosphonic acid is also found, indicating the enhancement of film packing. The hysteresis of the films is also an indicator of their packing; that is, as the ordering of the film increases, the hysteresis decreases. It can be seen that the hysteresis of the electrochemically prepared monolayers is slightly smaller than the chemically prepared monolayers. Taking into account the smoother surfaces used for chemisorption of the SAMs also points to the superior monolayers obtained by the electrochemically assisted method as compared to the chemisorbed approach. Furthermore, as the chain length increases, the hysteresis and error bars decrease. This can be attributed to the higher degree of order, more complete surface coverage, and somewhat higher packing density. In general, contact angles greater than 110° are typical of well-defined alkylphosphate SAMs,[46] indicating that hexylphosphonic acid does not form highly ordered monolayers.

XPS analysis was carried out on bare, hexylphosphonic, and decylphosphonic acids for both methods. The element composition obtained from low-resolution scans of hexylphosphonic acid is shown in Figure 2S. A clear difference is seen between the bare and coated samples in which the C signal increases, whereas the O, Ti, and P signals decrease accordingly. These trends all point to the formation of a layered coating where Ti is bound through the phosphonic moiety and the alkyl chain is oriented outward. The decrease in the Ti signal clearly suggests that the actively coated hexcylphosphonic acid monolayer is thicker than the passively coated hexylphosphonic acid monolayer, which is also supported by the difference in the P signal.

More information about the monolayers can be obtained from a careful analysis of high-resolution XPS scans. The C 1s spectrum, presented for the hexylphosphonic acid in both methods and the bare sample, is shown in Figure 3S. It can be seen that there is a clear difference between the substrate high-resolution spectrum and that of the monolayer-covered samples. The carbons found on the bare substrate are carbonate contaminations widely known on the titanium substrate, while the carbon signal of the covered samples is attributed mainly to the carbon of the aliphatic chain (285.0 eV).[21] It can be seen that the electrochemically prepared method gives rise to a higher intensity for the carbon main peak, indicating a higher content of molecules.

The high-resolution O 1s spectrum of chemically and electrochemically prepared hexylphosphonic acid is shown in Figure 3A. The figure shows several main contributions. A peak at 530.7 eV is related to the TiO_2 bond (passive 36.83%, FWHM = 1.05 eV; active 46.10%, FWHM = 0.8 eV);[10] that at 531.6 eV is related to P−O−Ti and P═O bonds (passive 59.05%, FWHM = 2 eV; active 44.65%, FWHM = 2 eV);[10] and that at 533.9 eV is related to the O−C bond (passive 4.12%, FWHM = 1.5 eV; active 9.25%, FWHM = 1.8 eV), which are considered to be surface contaminants.[47] These results can exclude binding modes between the SAMs and the titanium surface via the revealed bonds. In general, phosphonic acid does not suffer from homocondensation and can attach to the surface through hydrogen bonds, monodentate, bidentate, or tridentate configurations, or a mixture of these configurations.[48] Since no P−OH bond (532.6−533.6 eV[10]) was found in our results for the hexylphosphonic acid in both methods, we can

Table 2. Contact Angle Measurements of Bare, Chemisorbed, and Electrochemically Prepared Alkylphosphonic SAMs on the Ti Surface[a]

	chemisorbed			electrochemically prepared		
model tested	advancing contact angle (deg ± 0.1)	receding contact angle (deg ± 0.1)	hysteresis	advancing contact angle (deg ± 0.1)	receding contact angle (deg ± 0.1)	hysteresis
control	27.4 ± 0.7	9.4 ± 2.2		69.8 ± 3.9	49.3 ± 3.2	
hexylphosphonic acid	86.1 ± 7.4	60.9 ± 5.8	25.2 ± 9.4	94.0 ± 2.1	74.6 ± 5.8	19.40 ± 6.17
decylphosphonic acid	105.1 ± 4	92.3 ± 2.9	12.8 ± 4.94	112.7 ± 2.3	101.5 ± 1.9	11.2 ± 2.98
tetradecylphosphonic acid	110.4 ± 1.6	99.8 ± 2.5	10.6			
hexadecylphosphonic acid + 2 mM NaOH	108.5 ± 0.4	98.7 ± 1.2	9.8			

[a]The mean ± standard deviation of three measurements is presented.

dx.doi.org/10.1021/la404829b | Langmuir XXXX, XXX, XXX−XXX

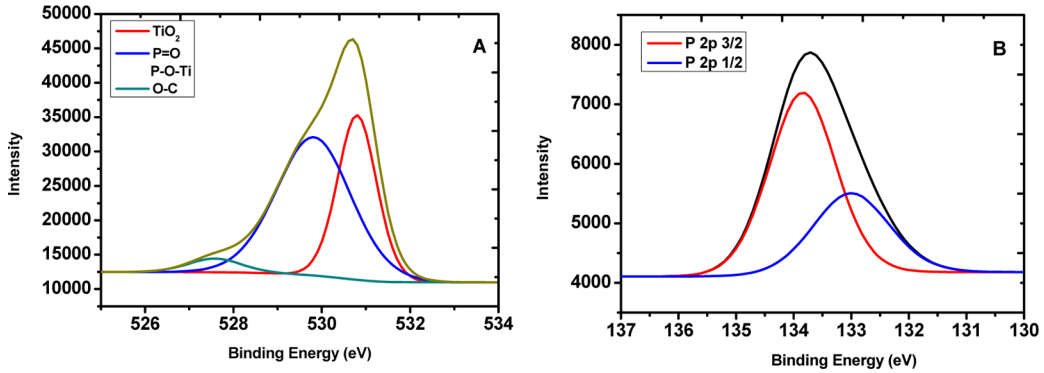

Figure 3. High-resolution XPS O 1s (A) and P 2p (B) spectra of chemisorbed hexylphosphonic acid SAMs.

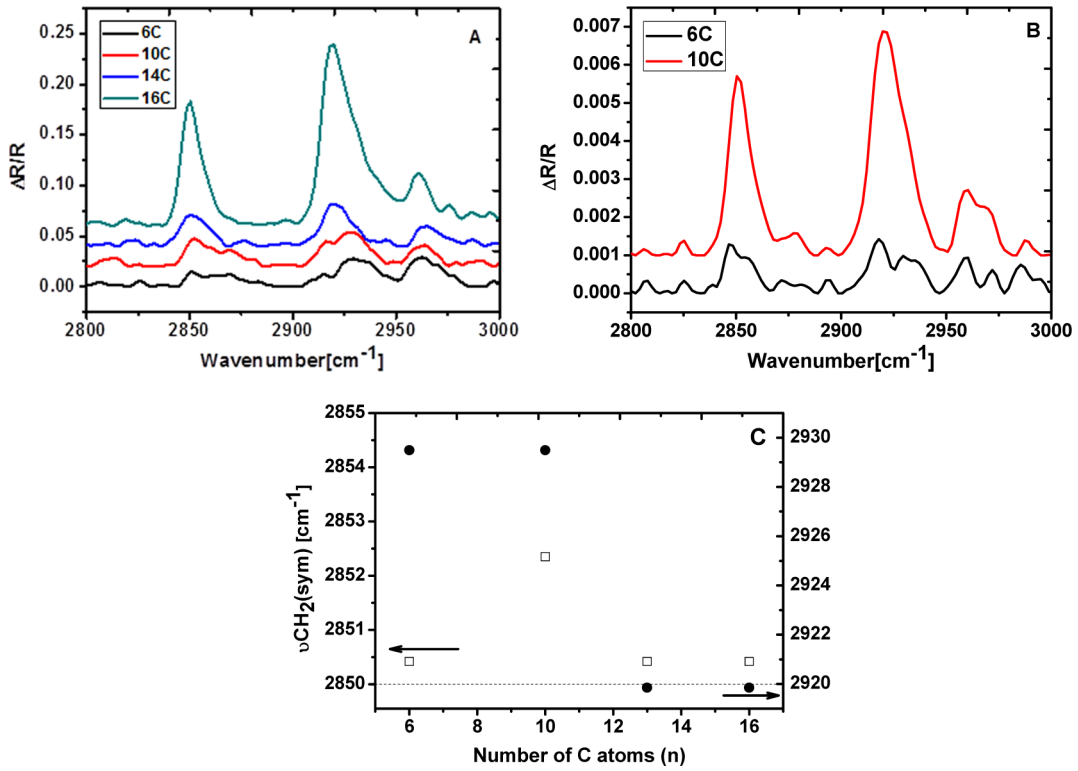

Figure 4. PM-IRRAS spectra in the C−H stretching region for the series of chemisorbed (A) and electrochemically prepared (B) phosphonate SAMs. 6C, 10C, 14C, and 16C stand for hexylphosphonic acid, decylphosphonic acid, tetradecylphosphonic acid, and hexadecylphosphonic acid, respectively. (C) Position of the methylene symmetric (open symbols) and antisymmetric (filled symbols) stretching modes in the chemisorbed method.

safely assume that the bond between the monolayer and the substrate is in either the bidentate or tridentate configuration, meaning that the monolayer is tightly adhered to the substrate with all valence electrons available to the phosphonate and no partially adsorbed layers on the surface. The detection of tridentate as the main binding mode in the case of alkylphosphonates and titanium was previously shown and studied.[49,50] The high-resolution spectrum of P 2p is shown in Figure 3B. It was fitted as a single doublet with P $2p_{3/2}$ at 133.7 ± 0.1 eV and P $2p_{1/2}$ with a binding energy difference of 0.81 eV and a fixed area ratio of 2:1 as reported before.[10]

Angle-resolved XPS was performed on octadecylphosphonic acid SAMs in the chemisorbed and electrochemically prepared methods at three different angles (see Tables 1S and 2S). In both tables, the oxygen and titanium signals decrease at more glancing takeoff angles. This is due to the decrease in the sampling depth with increasing takeoff angles, therefore resulting in a decreased signal from the underlying titanium dioxide layer. It is worth mentioning that the oxygen atoms within the phosphonate group contribute to the overall oxygen signal measured. However, it is evident that this contribution is minor (at least for small incident angles) as compared to that of the oxide layer. At the same time, the carbon and phosphorus signals increase at glancing takeoff angles in both systems. This means that the sampling depth, even for glancing angles, is still larger than the thickness of the organic layer. The ratio of the carbon signal to the phosphorus signal can be used to determine the molecular orientation. In theory, the phosphorus should be located at the TiO_2/SAM interface with the carbon chain oriented outward. The C/P ratio at more glancing takeoff angles for the chemisorbed layers does not change significantly and therefore does not provide evidence for ordering. On the

dx.doi.org/10.1021/la404829b | Langmuir XXXX, XXX, XXX−XXX

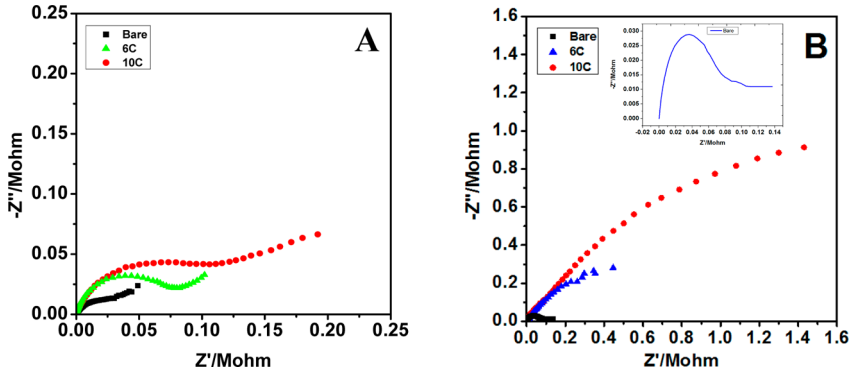

Figure 5. Nyquist plots of bare titanium vs titanium covered with alkylphosphonic acid. (A) Chemisorbed. (B) Electrochemically formed. The inset is a zoom-in for the bare sample.

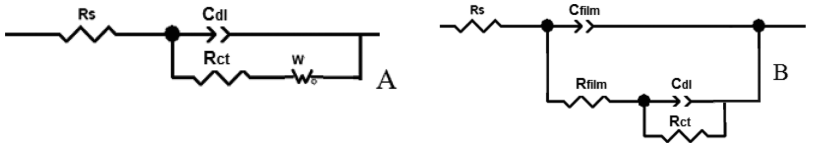

Figure 6. Equivalent circuits used to simulate the experimental data for SAMs deposited on Ti-6Al-4V, either chemically (A) or electrochemically (B).

Table 3. Parameters Obtained from Experimental Impedance Data Using the Equivalent Circuit in Figure 6A

	chemisorbed			electrochemically prepared		
	bare	6c	10c	bare	6c	10c
R_s [Ω]	100.8	97.04	95.61	104.1	311.2	99.02
R_{ct} [Ω]	30 281	76 908	83 210	73 169	7176	76 124
C_{dl} [F]	1.469×10^{-5}	3.75×10^{-6}	5.31×10^{-6}	5.61×10^{-6}	5.67×10^{-6}	1.75×10^{-6}
C_{film} [F]					1.00×10^{6}	4.25×10^{6}
R_{film} [Ω]					1.13×10^{6}	4.25×10^{6}

other hand, the decline in the C/P ratio in the electrochemical method is more substantial. This indicates that the organic monolayer is organized and the P is located below the C. This suggest that the angle between the molecules and the surface increases as compared to the chemisorbed assembly and a higher order of packing in the active method, which validates the information received from the different methods of charictarization.

Figure 4A,B presents the PM-IRRAS spectra, in the C−H vibrational region of 2800−3000 cm^{-1}, for evaporated titanium surfaces covered with chemisorbed SAMs (A) and electrochemically adsorbed SAMs (B). According to previous investigations, highly ordered aliphatic dense monolayers show stretching vibrations at 2960, 2920, and 2850 cm^{-1} for asymmetric and symmetric vibrations $\upsilon_{as}(-CH_3)$, $\upsilon_{as}(-CH_2)$, and $\upsilon_s(-CH_2)$, respectively. The most interesting feature of the chemisorbed series of spectra shown in Figure 4C is the shift in the positions of the methylene chains. These bands show a red shift to lower frequencies with increasing chain length, whereas the position of the methyl stretching bands remains almost invariant. The methylene stretching modes are known to be sensitive to the conformational order of alkyl chains (gauche defects), shifting to higher frequencies with increasing conformational disorder.[10] Figure 4C shows the position of the methylene stretching modes. Shorter chains appear at 2929 and 2852 cm^{-1}, indicating that the alkyl chains adopt a more ordered crystalline structure. The results are in agreement with the results described above. Furthermore, the gauche defects cause peak broadening of the symmetric and asymmetric CH_2 stretches.[51] It is evident that the shorter alkyls show broader peaks than the longer alkyls, implying a mixture of ordered and disordered adsorbents. Moreover, by comparing Figure 4A,B it is obvious that using the electrochemical method reduces gauche defects by narrowing the peaks.

Further insight into these systems was obtained by EIS, which allows an investigation of the interfaces in electrolyte solutions. It is worth mentioning that in this section the investigation was limited to short alkyl chains ($n < 10$). Long chains gave rise to obscure values, which are not easily interpreted. Impedance measurements were performed in a solution containing 1 mM $Ru(NH_3)_6^{3+}$ and 0.1 M KNO_3. Cyclic voltammetry was carried out before each experiment. The average of the oxidation and reduction peak potentials was then estimated to be $E^{0\prime}$ for the Ru complex. Figure 5 describes the EIS data in Nyquist plots for the chemisorbed and electrochemically adsorbed SAMs. Compared to the bare samples, both the chemically and electrochemically adsorbed films exhibit significantly higher impedance with correlation to the length of the alkyl chain. Moreover, the impedance for the electrochemically adsorbed SAMs is generally higher than that for the corresponding chemisorbed monolayers. The EIS data were further fitted with equivalent circuits as shown in Figure 6. The chemisorbed samples can be well fitted by the classical Randles circuit (Figure 6A). The obtained results are shown in Table 3. Considering the nonideal electrochemical interface due to the surface roughness, a constant phase element (CPE)

dx.doi.org/10.1021/la404829b | Langmuir XXXX, XXX, XXX−XXX

was used instead of the capacitance for fitting. It is seen that the charge-transfer resistance (R_{ct}), which is related to the active surface area of the electrodes, increases as the length of the alkyl chains in SAMs increases. This is in accordance with the trend shown in Figure 5A, suggesting that SAMs with longer alkyl chains form denser layers. However, the equivalent circuit for electrochemically prepared SAMs is more complex and consists of an additional (RC) relaxation in the high-frequency domain and in absence of the Warburg diffusion element (Figure 6B). We attribute this to the formation of an integrated barrier layer on the electrode surface, as it is not seen in the control sample electrochemically prepared from the electrolyte without alkylphosphonic acid. The high-frequency resistance, R_{film}, is related to the porosity of the barrier, while the corresponding C_{film} is associated with the thickness. The fitting results (Table 3) show that the electrochemically adsorbed decylphosphonic acid has a higher R_{film} and a lower C_{film} than the hexylphosphonic acid, indicating that the monolayer of decylphosphonic acid is denser and thicker. This is also in agreement with the trends in R_{ct} and C_{dl} values. Moreover, as compared to the chemisorbed monolayers, the electrochemically adsorbed layers have a significantly higher R_{ct}, suggesting that they provide higher coverage on the electrode surface. These results confirm that electrochemical adsorption is more efficient than the chemisorption method.

Figure 3S illustrates the effect of the chain length on the cyclic potentiodynamic polarization curve of Ti-6Al-4V coated with different alkylphosphonic acids. Prior to these tests, the open-circuit potential, E_{OCP}, was monitored for 1 h. At the vertex potential of 1 V, the scan was reversed in direction; the reverse scan, as seen in Figure 3S, is generally associated with higher potentials or lower current densities than in the forward scan, and the samples that do not follow this pattern are intersected with the forward scan in the passive region, thus creating a small hysteresis loop with high resistance to crevice corrosion. Similar behavior was reported and studied before for the Ti-6Al-4V alloy.[52] Table 4 summarizes the values of some

Table 4. E_{OCP} Obtained from Open-Circuit Potential Measurements, E_{corr} and i_{corr} Determined from the Potentiodynamic Polarization Curves, and Calculated η[a]

		chemisorbed SAMs				electroassisted SAMs	
	bare	6C	10C	14C	16C	6C	10C
E_{OCP} [mV]	−534	−136	−230	−300	−273	−195	−276
E_{corr} [mV]	−534	−201	−245	−337	−286	−270	−354
i_{corr} [μA/cm^2]	0.123	0.075	0.069	0.018	0.023	0.008	0.008
η		39%	44%	85%	81%	93%	93%

[a]Experiments were carried out in PBS at 37 °C.

important corrosion parameters, which were obtained through Tafel extrapolation. In all cases, E_{corr} deduced from the potentiodynamic measurements is somewhat more negative than E_{OCP} measured in the preliminary tests. In addition, the effect of the chain length is evident; as the chain length grows, the corrosion current densities i_{cor} are lowered both for the chemisorbed SAMs and for the electrochemically assisted SAMs. This indicates a decrease in the dissolution rate. Compared to the bare titanium surface, SAM-coated surfaces exhibit superior corrosion resistance, as evident by lower values of i_{corr}. These findings clearly indicate that the alkyl chains act as a corrosion barrier, in agreement with past publications.[53] The percentage of inhibition efficiencies (Table 4) was calculated using eq 3

$$\eta = \frac{i^0_{corr} - i_{corr}}{i^0_{corr}} \quad (3)$$

where i^0_{corr} and i_{corr} are the corrosion current densities in the absence and presence of SAMs, respectively. A clear trend in η can be seen as the chain length grows; the inhibition efficiency for long-chain SAMs is quite high. The lowered percentage for hexadecylposphonic acid can be explained by the formation of micelles in the aqueous solution.

The cyclic potentiodynamic polarization curves for electrochemically assisted SAMs are also shown in Figure 4S(F,G). We found that the curves are very similar to those for the chemisorbed samples, yielding comparable i_{corr} values, as shown in Table 4. Table 4 shows that in terms of kinetics, i_{corr} in the case of electrochemically assisted SAMs, for the same chain length, is lowered by an order in magnitude, indicating better corrosion protection.

CONCLUSIONS

Alkylphosphonic acid self-assembled monolayers with different chain lengths were assembled on Ti-6Al-4V via either chemisorption or electrochemical deposition. The bare and modified titanium alloys were studied by various surface techniques. It was found that long-chain acids form close-packed monolayers, resulting in more hydrophobic surfaces. Furthermore, the longer the chain, the more significant the reduction of electron transfer across the interface, thus influencing the corrosive behavior.

This study presents an electrochemical method for coating the surface with SAM at a shorter time constant as opposed to the chemisorption method that is widely used today. It was shown to have a performance similar to that for short-chain SAMs. The reason for the low time constant is entwined with the system mechanism and has mainly three justifications. First, when a positive voltage is applied to the surface, the amphiphiles in the vicinity of the electrode are polarized, allowing them to adhere to the surface in a better orientation. Thus, the cross-section of the molecule while arriving at the surface is lowered. Second, in viewing the adsorption mechanism of these amphiphiles, it is known that the time-determining step of non-cross-linked molecules is their assembly at the surface electrode, a process which has a high energy barrier.[54] Applying a potential to the surface allows us to overcome this energy barrier, and the time constant is lowered. In other words, when the surface energy is larger, the activation energy for organization is reduced. Finally, the surface texture has been proven before to make a major contribution to the organization of said molecules. For example, it has previously been shown that native TiO_2 and anodic TiO_2 adsorb siloxanes to different extents.[55] In our study, the different oxides may contribute to the changed time constant, being that anodized oxide is low in contaminants, which allows better surface coverage, and that its structure is smoother at these potentials.[6,56]

The chemisorbed and electrochemically assisted deposited SAMs exhibit similar performance to the short-chain SAMs and therefore can be considered to be equivalent methods. Taking

dx.doi.org/10.1021/la404829b | Langmuir XXXX, XXX, XXX−XXX

into account that the electrochemical deposition is faster, which allows better control of the interface between the monolayer and the substrate, and shows higher corrosion resistance, we conclude that this method is superior for assembling this type of SAM. Further work along this line and using bifunctional monolayers is in progress.

■ ASSOCIATED CONTENT

Supporting Information

Effect of the applied potential on the electron-transfer blocking properties of a decylphosphonic acid SAM. Angle-dependent XPS compositional results of the decylphosphonic acid monolayer for the chemisorbed and electrochemically prepared methods. Atomic composition (XPS) of the bare titanium and that coated with hexylphosphonic acid for both methods. High-resolution XPS C 1s spectra of bare hexylphosphonic acid SAMs for both the chemisorbed and electrochemically prepared methods. Potentiodynamic polarization curves of Ti-6Al-4V. This material is available free of charge via the Internet at http://pubs.acs.org.

■ AUTHOR INFORMATION

Corresponding Author

*E-mail: daniel.mandler@mail.huji.ac.il. Tel: +972 2 6585831. Fax: +972 2 6585319.

Notes

The authors declare no competing financial interest.

■ ACKNOWLEDGMENTS

This work was partially funded by the German-Israeli Foundation for Scientific Research and Development (GIF research grant no. 1074-49.10/2009). The Harvey M. Krueger Family Center for Nanoscience and Nanotechnology of the Hebrew University is also acknowledged.

■ ABBREVIATIONS

SAMs, self-assembled monolayers; RGD, Arg-Gly-Asp; PBS, phosphate-buffered saline; DI, deionized; RE, reference electrode; EIS, electrochemical impedance spectroscopy; PM-IRRAS, polarization modulation infrared reflection absorption spectroscopy; FTIR, Fourier transform infrared; LIA, lock-in amplifier; XPS, X-ray photoelectron spectroscopy; CV, cyclic voltammetry; SCE, saturated calomel electrode; 6C, hexylphosphonic acid; 10C, decylphosphonic acid; 14C, tetradecylphosphonic acid; 16C, hexadecylphosphonic acid; CPE, constant phase element

■ REFERENCES

(1) Eliaz, N. *Applications of Electrochemistry and Nanotechnology in Biology and Medicine I*; Modern Aspects of Electrochemistry, no. 52; Springer: New York, 2011.

(2) Sittig, C.; Textor, M.; Spencer, N. D.; Wieland, M.; Vallotton, P. H. Surface Characterization of Implant Materials cp Ti, Ti-6Al-7Nb and Ti-6Al-4V with Different Pretreatments. *J. Mater. Sci.: Mater. Med.* **1999**, *10*, 35−46.

(3) Eliaz, N. In *Corrosion Science and Technology: Mechanism, Mitigation and Monitoring*; Mudali, U. K., Raj, B., Eds.; Narosa Publishing House: New Delhi, 2008; Chapter 12, pp 356−397.

(4) Kerber, S. J. Bioreactivity of Titanium Implant Alloys. *J. Vac. Sci. Technol., A* **1995**, *13*, 2619−2623.

(5) Liu, Q.; Ding, J.; Mante, F. K.; Wunder, S. L.; Baran, G. R. The Role of Surface Functional Groups in Calcium Phosphate Nucleation on Titanium Foil: a Self-Assembled Monolayer Technique. *Biomaterials* **2002**, *23*, 3103−3111.

(6) Liu, X. Y.; Chu, P. K.; Ding, C. X. Surface Modification of Titanium, Titanium Alloys, and Related Materials for Biomedical Applications. *Mater. Sci. Eng. R* **2004**, *47*, 49−121.

(7) Navarro, M.; Michiardi, A.; Castaño, O.; Planell, J. A. Biomaterials in Orthopaedics. *J. R. Soc. Interface* **2008**, *5*, 1137−1158.

(8) Xiao, S. J.; Textor, M.; Spencer, N. D.; Wieland, M.; Keller, B.; Sigrist, H. Immobilization of the Cell-Adhesive Peptide Arg-Gly-Asp-Cys (RGDC) on Titanium Surfaces by Covalent Chemical Attachment. *J. Mater. Sci.: Mater. Med.* **1997**, *8*, 867−872.

(9) Adadi, R.; Zorn, G.; Brener, R.; Gotman, I.; Gutmanas, E. Y.; Sukenik, C. N. Phosphonate-Anchored Thin Films on Titanium and Niobium Oxide Surfaces: Fabrication and Characterization. *Thin Solid Films* **2010**, *518*, 1966−1972.

(10) Spori, D. M.; Venkatarman, N. V.; Tosatti, S. G. P.; Durmaz, F.; Spencer, N. D.; Zürcher, S. Influence of Alkyl Chain Length on Phosphate Self-Assembled Monolayers. *Langmuir* **2007**, *23*, 8053−8060.

(11) Clair, S.; Variola, F.; Kondratenko, M.; Jedrzejowski, P.; Nanci, A.; Rosei, F.; Perepichka, D. F. Self-Assembled Monolayer of Alkanephosphoric Acid on Nanotextured Ti. *J. Chem. Phys.* **2008**, *128*, 144705.

(12) Mann, J. R.; Nevins, J. S.; Soja, G. R.; Wells, D. D.; Levy, S. C.; Marsh, D. A.; Watson, D. F. Influence of Solvation and the Structure of Adsorbates on the Kinetics and Mechanism of Dimerization-Induced Compositional Changes of Mixed Monolayers on TiO_2. *Langmuir* **2009**, *25*, 12217−12228.

(13) Soja, G. R.; Mann, J. R.; Watson, D. F. Temporal Evolution of the Composition of Mixed Monolayers on TiO_2 Surfaces: Evidence for a Dimerization-Induced Chelate Effect. *Langmuir* **2008**, *24*, 5249−5252.

(14) Song, Y. Y.; Hildebrand, H.; Schmuki, P. Optimized Monolayer Grafting of 3-aminopropyltriethoxysilane onto Amorphous, Anatase and Rutile TiO_2. *Surf. Sci.* **2010**, *604*, 346−353.

(15) Tan, G.; Zhang, L.; Ning, C.; Liu, X. Liao, j. Preparation and Characterization of APTES Films on Modification Titanium by SAMs. *Thin Solid Films* **2011**, *519*, 4997−5001.

(16) Zuo, J.; Torres, E. Comparison of Adsorption of Mercaptopropyltrimethoxysilane on Amphiphilic TiO_2 and Hydroxylated SiO_2. *Langmuir* **2010**, *26*, 15161−15168.

(17) Ajami, E.; Aguey-Zinsou, K. F. Formation of OTS Self-Assembled Monolayers at Chemically Treated Titanium Surfaces. *J. Mater. Sci.: Mater. Med.* **2011**, *22*, 1813−1824.

(18) Hahner, G.; Hofer, R.; Klingenfuss, I. Order and Orientation in Self-Assembled Long Chain Alkanephosphate Monolayers Adsorbed on Metal Oxide Surfaces. *Langmuir* **2001**, *17*, 7047−7052.

(19) HailuTaffa, D.; Kathiresan, M.; Walder, L. Tuning the Hydrophilic, Hydrophobic, and Ion Exchange Properties of Mesoporous TiO_2. *Langmuir* **2009**, *25*, 5371−5379.

(20) Balaur, E.; Macak, J. M.; Taveira, L.; Schmuki, P. Tailoring the Wettability of TiO_2 Nanotube Layers. *Electrochem. Commun.* **2005**, *7*, 1066−1070.

(21) Adden, N.; Gamble, L. J.; Castner, D. G.; Hoffmann, A.; Gross, G.; Menzel, H. Phosphonic Acid Monolayers for Binding of Bioactive Molecules to Titanium Surfaces. *Langmuir* **2006**, *22*, 8197−8204.

(22) Gawalt, E. S.; Avaltron, M. J.; Danahy, M. P.; Silverman, B. M.; Hanson, E. L.; Midwood, K. S.; Schwarzbauer, J. E.; Schwartz, J. Bonding Organics to Ti Alloys: Facilitating Human Osteoblast Attachment and Spreading on Surgical Implant Materials. *Langmuir* **2003**, *19*, 200−204.

(23) Bozzini, S.; Petrini, P.; Tanzi, M. C.; Zürcher, S.; Tosatti, S. Poly(ethylene glycol) and Hydroxy Functionalized Alkane Phosphate Mixed Self-Assembled Monolayers to Control Nonspecific Adsorption of Proteins on Titanium Oxide Surfaces. *Langmuir* **2010**, *26*, 6529−6534.

(24) Yamaguchi, Y.; Adachi, M.; Iijima, M.; Wakamatsu, N.; Kamemizu, H.; Omoto, S.; Doi, Y. Thin Carbonate Apatite Layer

Biomimetically-Coated on SAM-Ti Substrate Surfaces. *J. Ceram. Soc. Jpn.* **2010**, *118*, 458−461.
(25) Lei, L.; Li, C.; Yang, P.; Huang, N. Photo-Immobilized Heparin Micropatterns on Ti-O Surface: Preparation, Characterization, and Evaluation *in-vitro*. *J. Mater. Sci.* **2011**, *46*, 6772−6782.
(26) Xiao, S. J.; Textor, M.; Spencer, N. D. Covalent Attachment of Cell-Adhesive, (Arg-Gly-Asp)-Containing Peptides to Titanium Surfaces. *Langmuir* **1998**, *14*, 5507−5516.
(27) Adolphi, B.; Jahne, E.; Busch, G.; Cai, X. Characterization of the Adsorption of Omega-(thiophene-3-yl alkyl) Phosphonic Acid on Metal Oxides with AR-XPS. *Anal. Bioanal. Chem.* **2004**, *379*, 646−652.
(28) Silverman, B. M.; Wieghaus, K. A.; Schwartz, J. Comparative Properties of Siloxane vs. Phosphonate Monolayers on a Key Titanium Alloy. *Langmuir* **2005**, *21*, 225−228.
(29) Weisshaar, D. E.; Lamp, B. D.; Porter, M. D. Thermodynamically Controlled Electrochemical Formation of Thiolate Monolayers at Gold - Characterization and Comparison to Self-Assembled Analogs. *J. Am. Chem. Soc.* **1992**, *114*, 5860−5862.
(30) Hatchett, D. W.; Uibel, R. H.; Stevenson, K. J.; Harris, J. M.; White, S. W. Electrochemical Measurement of the Free Energy of Adsorption of n-Alkanethiolates at Ag(111). *J. Am. Chem. Soc.* **1998**, *120*, 1062−1069.
(31) Stevenson, K. J.; Mitchell, M.; White, H. S. Oxidative Adsorption of n-Alkanethioiates at Mercury. Dependence of Adsorption Free Energy on Chain Length. *J. Phys. Chem. B* **1998**, *102*, 1235−1240.
(32) Hatchett, D. W.; Stevenson, K. J.; Lacy, W. B.; Harris, J. M.; White, H. S. Electrochemical Oxidative Adsorption of Ethanethiolate on Ag(111). *J. Am. Chem. Soc.* **1997**, *119*, 6596−6606.
(33) Ron, H.; Rubinstein, I. Self-Assembled Monolayers on Oxidized Metals. 3. Alkylthiol and Dialkyl Disulfide Assembly on Gold Under Electrochemical Conditions. *J. Am. Chem. Soc.* **1998**, *120*, 13444−13452.
(34) Brett, C. M. A.; Kresak, S.; Hianik, T.; Brett, M. O. Studies on Self-Assembled Alkanethiol Monolayers Formed at Applied Potential on Polycrystalline Gold Electrodes. *Electroanalysis* **2003**, *15*, 557−565.
(35) Bengio, S.; Fonticelli, M.; Benitez, G.; Creus, A. H.; Carro, P.; Ascolani, H.; Zampieri, G.; Blum, B.; Salvarezza, R. C. Electrochemical Self-Assembly of Alkanethiolate Molecules on Ni(111) and Polycrystalline Ni Surfaces. *J. Phys. Chem. B* **2005**, *109*, 23450−23460.
(36) Shustak, G.; Domb, A. J.; Mandler, D. Preparation and Characterization of n-Alkanoic Acid Self-Assembled Monolayers Adsorbed on 316L Stainless Steel. *Langmuir* **2004**, *20*, 7499−7506.
(37) Zhang, H. P.; Romero, C.; Baldelli, S. Preparation of Alkanethiol Monolayers on Mild Steel Surfaces Studied with Sum Frequency Generation and Electrochemistry. *J. Phys. Chem. B* **2005**, *109*, 15520−15530.
(38) Weber, C. R.; Dick, L. F. P.; Benitez, G.; Vela, M. E.; Salvarezza, R. C. Electrochemically Induced Self-Assembly of Alkanethiolate Adlayers on Carbon Steel in Aqueous Solutions. *Electrochim. Acta* **2009**, *54*, 4817−4821.
(39) Petrovic, Z.; Metikos-Hukovic, M.; Harvey, J.; Omanovic, S. Enhancement of Structural and Charge-Transfer Barrier Properties of n-Alkanethiol Layers on a Polycrystalline Copper Surface by Electrochemical Potentiodynamic Polarization. *Phys. Chem. Chem. Phys.* **2010**, *12*, 6590−6593.
(40) Maho, A.; Denayer, J.; Delhalle, J.; Mekhalif, Z. Electro-Assisted Assembly of Aliphatic Thiol, Dithiol and Dithiocarboxylic Acid Monolayers on Copper. *Electrochim. Acta* **2011**, *56*, 3954−3962.
(41) Oya, K.; Tanaka, Y.; Saito, H.; Kurashima, K.; Nogi, K.; Tsutsumi, H.; Tsutsumi, Y.; Doi, H.; Nomura, N.; Hanawa, T. Calcification by MC3T3-E1 Cells on RGD Peptide Immobilized on Titanium Through Electrodeposited PEG. *Biomaterials* **2009**, *30*, 1281−1286.
(42) Muskal, N.; Mandler, D. Thiol Self-Assembled Monolayers on Mercury Surfaces: The Adsorption and Electrochemistry of Omega-Mercaptoalkanoic Acids. *Electrochim. Acta* **1999**, *45*, 537−548.
(43) Yan, S. G.; Hupp, J. T. Semiconductor-Based Interfacial Electron-Transfer Reactivity: Decoupling Kinetics from pH-Dependent Band Energetics in a Dye-Sensitized Titanium Dioxide Aqueous Solution System. *J. Phys. Chem.* **1996**, *100*, 6867−6870.
(44) Boschloo, G.; Fitzmaurice, D. Electron Accumulation in Nanostructured TiO_2 (Anatase) Electrodes. *J. Electrochem. Soc.* **2000**, *147*, 1117−1123.
(45) Kosolapoff, G. M. Chemistry of Aliphatic Phosphonic Acids. II. Dielectric Constants and Viscosity of Some Higher Alkylphosphonates. *J. Am. Chem. Soc.* **1954**, *76*, 615−617.
(46) Hofer, R.; Textor, M.; Spencer, N. D. Alkyl Phosphate Monolayers, Self-Assembled from Aqueous Solution onto Metal Oxide Surfaces. *Langmuir* **2001**, *17*, 4014−4020.
(47) Viornery, C.; Chevolot, Y.; Leonard, D.; Aronsson, B.; Pechy, P.; Matheiu, H. J.; Descounts, P.; Gratzel, M. Surface Modification of Titanium with Phosphonic Acid to Improve Bone Bonding: Characterization by XPS and ToF-SIMS. *Langmuir* **2002**, *18*, 2582−2589.
(48) Thissen, P.; Vega, A.; Peixoto, T.; Chabal, Y. J. Controlled, Low-Coverage Metal Oxide Activation of Silicon for Organic Functionalization: Unraveling the Phosphonate Bond. *Langmuir* **2012**, *28*, 17494−17505.
(49) Guerrero, G.; Mutin, P. H.; Vioux, A. Anchoring of Phosphonate and Phosphinate Coupling Molecules on Titania Particles. *Chem. Mater.* **2001**, *13*, 4367−4373.
(50) Randon, J.; Blanc, P.; Paterson, R. Modification of Ceramic Membrane Surfaces Using Phosphoric-Acid and Alkyl Phosphonic-Acids and its Effects on Ultrafiltration of BSA Protein. *J. Membr. Sci.* **1995**, *98*, 119−129.
(51) Bittner, A. M.; Epple, M.; Kuhnke, K.; Hourient, R.; Heusler, A.; Vogel, H.; Seitsonen, A. P.; Kern, K. Conformations of an Amino-Amido-Thiolate Self-Assembled Layer on Gold in Air and in Electrolytes. *J. Electroanal. Chem.* **2003**, *550*, 113−124.
(52) Bhola, R.; Bhola, S. M.; Mishra, B.; Ayers, R.; Olson, D. L. In *Electrochemical Characteristics of Titanium and its Alloys in Phosphate Buffer Saline*; Medical Device Materials V; Proceedings from the Materials & Processes for Medical Devices Conference, ASM International, Minneapolis, MN, August 10−12, 2009, Vol. *8*, pp 52−59.
(53) Zamborini, F. P.; Crooks, R. M. Corrosion Passivation of Gold by n-Alkanethiol Self-Assembled Monolayers: Effect of Chain Length and End Group. *Langmuir* **1998**, *14*, 3279−3286.
(54) Ulman, A. Formation and Structure of Self-Assembled Monolayers. *Chem. Rev.* **1996**, *96*, 1533−1554.
(55) Killian, M. S.; Gnichwitz, J. F.; Hirsch, A.; Schmuki, P.; Kunze, J. ToF-SIMS and XPS Studies of the Adsorption Charicteristics of a Zn-porphyrin on TiO_2. *Langmuir* **2010**, *26*, 3531−3538.
(56) Diamanti, M. V.; Pedeferri, M. P. Effect of Anodic Oxidation Parameters on the Titanium Oxides Formation. *Corros. Sci.* **2007**, *49*, 939−948.